

Experimental verification of methods for solving the two-dimensional Laplace equation for electric potential given Dirichlet boundary conditions

Evan J. Arena^{1,2,*}, Aaron Seymour¹, Anthony Bader¹, and Jacob Brooks¹

1. State University of New York at Stony Brook,
Department of Physics and Astronomy
and
2. Brookhaven National Laboratory,
Baryon Mapping eXperiment (BMX)

(SABB Collaboration)
(Dated: 24 November 2015)

We investigate three methods for solving Laplace's equation in a closed two-dimensional plane given Dirichlet boundary conditions. The region is split into a grid in order to find the electrical potential at the various gridpoints. These values are measured experimentally in the lab, calculated by means of a numerical approximation method, and found using an exact theoretical solution. They are then compared to one another under confidence intervals.

Usage: This is the final project for the Stony Brook University Fall 2015 PHY 301 course taught by Prof. Eden Figueroa.

I. INTRODUCTION

Using the Laplace equation in order to determine the electric field of a configuration is not an intuitive approach. Generally, we can describe the electric field of a static charge distribution as

$$\mathbf{E}(\mathbf{r}) = \frac{1}{4\pi\epsilon_0} \int \frac{\rho(\mathbf{r}')}{\mathcal{R}^2} \hat{\mathcal{R}} d^3 r' \quad (1)$$

where the separation vector $\mathcal{R} = \mathbf{r} - \mathbf{r}'$ points from the location of the localized charge density $\rho(\mathbf{r}')$ to the point of interest. This becomes an inefficient approach when we are interested in finding the electric field over a region of space, so we employ Gauss' law

$$\nabla \cdot \mathbf{E} = \frac{\rho}{\epsilon_0} \quad (2)$$

It is useful to define a scalar electric potential such that

$$\mathbf{E} = -\nabla V \quad (3)$$

when used, equation (2) becomes

$$\nabla^2 V = -\frac{\rho}{\epsilon_0} \quad (4)$$

which is Poisson's equation. In regions where there is no localized charge, Poisson's equation becomes the Laplace equation:

$$\nabla^2 V = 0 \quad (5)$$

The solution to this equation, which will be found later in this manuscript, can be used to find the electric potential function within the region. This is one approach, referred to as the analytical one. We will employ two other methods for finding this potential function: an experimental one and a numerical approximation. It will be clear that we are dealing with the two-dimensional Laplace equation in a rectangular region with Dirichlet boundary conditions in the discussion of the experimental setup.

II. EXPERIMENTAL METHOD

A. Experimental setup

The area that was probed consisted of a carbon sheet sectioned into a 20 x 25 grid with 1cm spacing clamped into place. The edges of this sheet were coated with conductive paint of roughly 1cm width. The left, right, and bottom sides were continuously painted into one conductor, while the top was separated (FIG 1).

The three-sided continuous strip was connected to the ground terminal of a Lambda LL-902-OV regulated power supply via banana cable and alligator clips. Since the ground is not ideal, we connect all three sides to the ground rather than just one. In a similar fashion, the positive terminal was connected to the top conductor, supplying a potential in volts $V_0 = 9.020 \pm 0.005V$ as measured by a probe connected to a Lutron DV-101 DC Digital Voltmeter that was connected in series into the circuit both via banana cables and alligator clips.

* electronic mail: evan.arena@stonybrook.edu

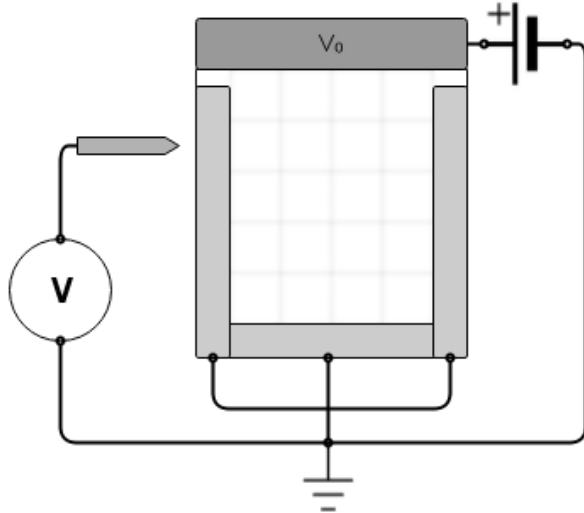


FIG. 1.

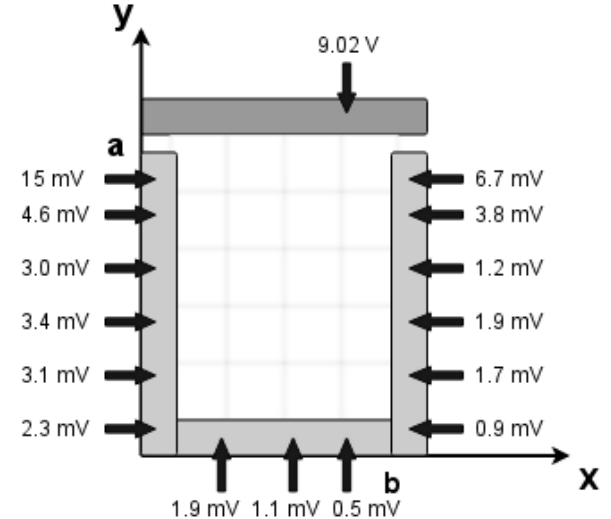


FIG. 2.

B. Methodology

In order to effectively quadruple the amount of points we could measure from this 20×25 grid, we probed every half cm rather than just at the marked 1 cm grid-points. Before we probed the grid, we first measured the potential along various points on the conductors to take into account the imperfections in the paint and the ground. With the power supply set to 9V, we measured $V_0 = 9.020 \pm 0.005$ V on the top grid, as previously mentioned. We found that the value along the ground fluctuated based on position and measured various values in milliVolts as shown in (FIG 2). This lead to an uncertainty that will be discussed at a later point in this manuscript.

We then measured the potential on our imaginary 38 x 49 grid and carefully recorded the data into a shared Google Documents spreadsheet. In our group of four individuals, we would have one group member probe each point on the grid once and read off the potential values given on the voltmeter, with another member watching both the placement of the probe on the grid and checking the value that appeared on the voltmeter. A third member would record the data into the spreadsheet, while the fourth would ensure that the correct values were input in the correct location while watching the spreadsheet from a separate terminal. Near the top conductor V_0 , the potential was on the order of 1V and near the bottom of the grid on the order of 0.1V, so we used the 2V and 0.2V settings on the voltmeter, respectively. We chose three distinct points on the grid corresponding to $(x, y) = (4, 44), (18, 24), (18, 3)$ when you impose an xy axis along the grid as depicted in (FIG 2). These points were measured an additional 20 times (21 total) in order to get a good estimate for uncertainty.

C. Data Analysis

From our data, we will investigate possible sources of uncertainty in our measurements. In the lab, as previously mentioned, we measured three gridpoints a total of $N = 21$ times. We found an average for each of these three data points by

$$V_{N,\alpha} = \frac{1}{N} \sum_{i=1}^N V_i \quad (6)$$

where $V_{N,\alpha}$ represents the averages for the three gridpoints ($\alpha = 1, 2, 3$). We then found the standard deviation for each of the three points by

$$\delta_{N,\alpha} = \sqrt{\frac{\sum_{i=1}^N (V_i - V_{N,\alpha})^2}{N(N-1)}} \quad (7)$$

and the average standard deviation

$$\bar{\delta} = \frac{1}{\alpha} \sum_{i=1}^{\alpha} \delta_{N,\alpha} \quad (8)$$

In doing so, we found that $\bar{\delta} = 0.006$ V, but to be conservative, we will take the largest of the three individual standard deviations $\delta_{N,1} = 0.0158$ V to be the uncertainty with which we are dealing. Now, in reality, this value should account for all possible uncertainty in the experiment. Measuring these three points multiple times should cover imperfections in the carbon paper, the probe not landing exactly in the desired location along the grid for every measured point, and perhaps even uncertainty in voltmeter readings, as well as

the fluctuations measured on the three-sided grounded conductor (FIG 2). For the last two of four possible uncertainties, we are assuming that measuring these points multiple times averages out the uncertainty in the voltmeter itself, but we could again be conservative and claim that it does not necessarily do so. We noticed that on the 2V setting of the voltmeter, each measured gridpoint value appearing on the screen would fluctuate by about 0.01V. On the 0.2V setting, this corresponded to a fluctuation of 0.001V. Being conservative, we take the uncertainty in the voltmeter to be that of the 2V setting: $\delta_{VOLT} = 0.01V$. If we also decide to directly account for the fluctuations measured on the grounded conductor, we find that by the standard deviation process, these values fluctuate by $\delta_{GROUND} = 0.00087$. We get a total uncertainty

$$\delta_{TOT} = \delta_{N,1} + \delta_{VOLT} + \delta_{GROUND} \quad (9)$$

of $\delta_{TOT} = 0.02667V$. Even with this very conservative value for uncertainty, we found that confidence lines for the contour plot of the experimental data (FIG 5) lie within the average contour lines and are therefore negligible.

D. Experimental Results

After organizing the data, we were able to construct a three-dimensional point plot (FIG 3) and surface plot (FIG 4) using Mathematica:

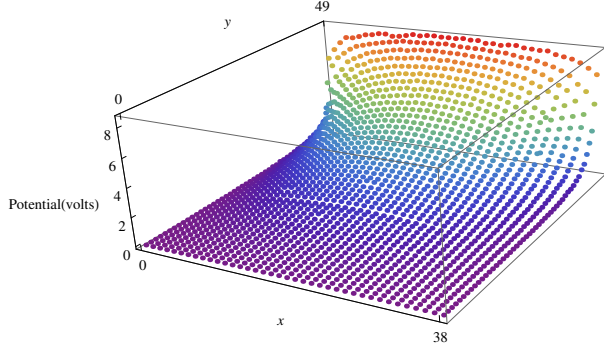


FIG. 3. Experimental list plot

After we carefully considered uncertainty, we were able to create an appropriate countour plot as well (FIG 5).

III. ANALYTICAL METHOD

A. Theory

The goal of the analytical method is to find the potential in the region by use of a theoretical formula. Since

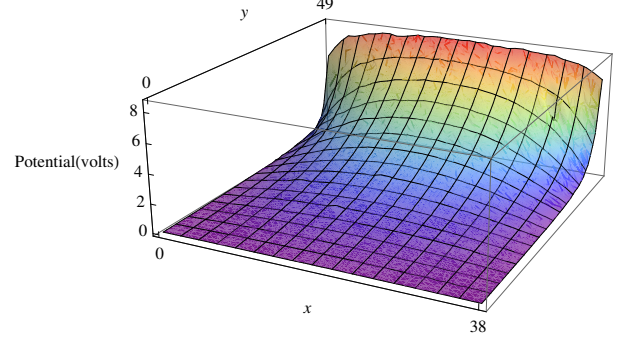


FIG. 4. Experimental surface plot

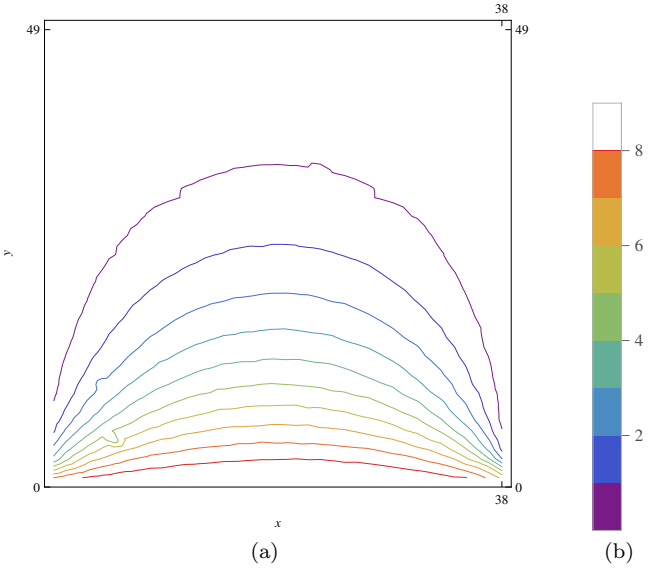


FIG. 5. Experimental contour plot

there is no localized charge, we must proceed by finding the general solution to Laplace's equation (Eq. 5). Since we find ourselves dealing with a two-dimensional rectangular domain, Eq. 5 becomes

$$\frac{\partial^2 V}{\partial x^2} + \frac{\partial^2 V}{\partial y^2} = 0 \quad (10)$$

We use separation of variables to look for solutions in the form of a product of two single variable functions

$$V(x, y) = X(x)Y(y) \quad (11)$$

Using this as a guess solution, Eq. 10 becomes

$$Y \frac{d^2 X}{dx^2} + X \frac{d^2 Y}{dy^2} = 0 \quad (12)$$

Now we separate the variables by dividing by Eq. 11

$$\frac{1}{X} \frac{d^2 X}{dx^2} + \frac{1}{Y} \frac{d^2 Y}{dy^2} = 0 \quad (13)$$

We see that the first term now entirely depends on x and the second on y . We have an equation of the form

$$f(x) + g(y) = 0 \quad (14)$$

We now realize that if we were to vary x and hold y constant, or vice versa, the LHS of Eq. 14 would no longer equal zero; therefore, f and g must both be constant. From Eq. 13 we define

$$\frac{1}{X} \frac{d^2 X}{dx^2} \equiv C_1 \quad \text{and} \quad \frac{1}{Y} \frac{d^2 Y}{dy^2} \equiv C_2 \quad (15)$$

where

$$C_1 + C_2 = 0 \quad (16)$$

For our purposes, we need C_1 negative and C_2 positive for reasons that will become apparent shortly. We are then left with two ordinary differential equations:

$$\frac{1}{X} \frac{d^2 X}{dx^2} = -k^2 \quad (17)$$

$$\frac{1}{Y} \frac{d^2 Y}{dy^2} = k^2 \quad (18)$$

Then the general solution for Eq. 17 is

$$X(x) = A \sin(kx) + B \cos(kx) \quad (19)$$

And for Eq. 18

$$Y(y) = C e^{ky} + D e^{-ky} \quad (20)$$

Now it is time to take the two general solutions given by Eq. 19 and Eq. 20 into specific solutions based on the Dirichlet boundary conditions of our experiment, as shown in (FIG 6)

or more succinctly,

$$\left. \begin{array}{l} \text{(i)} \quad V(x = a, y = 0) = 0 \\ \text{(ii)} \quad V(x = b, y = 0) = 0 \\ \text{(iii)} \quad V(x, y = 0) = 0 \\ \text{(iv)} \quad V(x, y = a) = V_0 \end{array} \right\} \quad (21)$$

Using boundary condition (i), Eq. 19 becomes

$$X(x = 0) = 0 = A \sin(x = 0) + B \cos(x = 0) = B \quad (22)$$

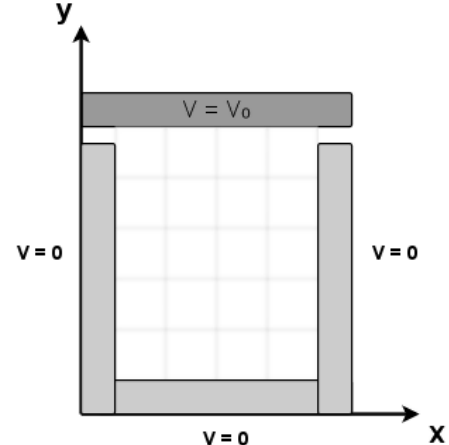


FIG. 6. Dirichlet boundary conditions

Since if $V = 0$, Eq. 11 requires that $X(x) = 0$. Now, Eq. 22 tells us that $B = 0$, so Eq. 19 becomes

$$X(x) = A \sin(kx) \quad (23)$$

We find A by imposing boundary condition (ii) on Eq. 23

$$X(x = b) = 0 = A \sin(k(x = b)) = A \sin(kb) \quad (24)$$

Eq. 24 implies that

$$kb = \pi, 2\pi, 3\pi, \dots \equiv n\pi \quad (25)$$

where $n = 1, 2, 3, \dots$, since $n = 0$ implies that the potential is zero everywhere, and is hence no good. At this point, it should be apparent why C_1 was chosen negative and C_2 positive: if Y were sinusoidal and X exponential, we could have not arranged the appropriate boundary conditions given by Eq. 21. Eq. 25 then becomes

$$k = \frac{n\pi}{b} \quad (26)$$

With Eq. 26, and recognizing that $B = 0$, Eq. 19 becomes

$$X(x) = A \sin\left(\frac{n\pi x}{b}\right) \quad (27)$$

Now we impose boundary condition (iii) on Eq. 20

$$Y(y = 0) = 0 = C e^{k(y=0)} + D e^{-k(y=0)} = C + D \quad (28)$$

Clearly

$$C = -D \quad (29)$$

With Eq. 29, Eq. 19 becomes

$$Y(y) = Ce^{ky} - C^{-ky} \quad (30)$$

We recognize that Eq. 30 is a form of the hyperbolic sine function written in exponential form and is therefore

$$Y(y) = 2C \sinh(ky) \quad (31)$$

With Eq. 26, Eq. 30 becomes

$$Y(y) = 2C \sinh\left(\frac{n\pi y}{b}\right) \quad (32)$$

Now, using Eq. 27 and Eq. 32, Eq. 11 becomes

$$V(x, y) = \sum_{n=1}^{\infty} \left[A \sin\left(\frac{n\pi x}{b}\right) \right] \left[2C \sinh\left(\frac{n\pi y}{b}\right) \right] \quad (33)$$

We let $C_n \equiv 2AC$, then Eq. 33 becomes

$$V(x, y) = \sum_{n=1}^{\infty} C_n \sin\left(\frac{n\pi x}{b}\right) \sinh\left(\frac{n\pi y}{b}\right) \quad (34)$$

Now we need to find C_n . We first impose boundary condition (iv), and Eq. 34 becomes

$$V(x, y=a) = V_0 = \sum_{n=1}^{\infty} C_n \sin\left(\frac{n\pi x}{b}\right) \sinh\left(\frac{n\pi a}{b}\right) \quad (35)$$

We recognize Eq. 35 as a Fourier sine series and hence apply Fourier's trick. We see that for even values of n, the RHS of Eq. 34

$$C_n \sin\left(\frac{n\pi x}{b}\right) \sinh\left(\frac{n\pi a}{b}\right) = 0 \quad (36)$$

And for odd values of n,

$$C_n \sinh\left(\frac{n\pi a}{b}\right) = \frac{4V_0}{n\pi} \quad (37)$$

Eq. 37 then tells us that

$$C_n = \frac{4V_0}{n\pi \sinh\left(\frac{n\pi a}{b}\right)} \quad (38)$$

With Eq. 38 and recognizing that $n = 1, 3, 5, \dots$, Eq. 34 gives us the two-dimensional solution to Laplace's equation $V(x, y)$ given our Dirichlet boundary conditions:

$$V(x, y) = \frac{4V_0}{\pi} \sum_{n=1}^{\infty} \frac{\sin\left(\frac{n\pi x}{b}\right) \sinh\left(\frac{n\pi y}{b}\right)}{n \sinh\left(\frac{n\pi a}{b}\right)} \quad (39)$$

This is guaranteed to be the only solution as per the uniqueness theorems.

B. Application

Now that we have the solution to Laplace's equation, we must use it to calculate the value of the potential at each point in order to compare to our experimental measurements. We wrote a Fortran code that begins by defining a matrix to act as our potential gradient. Its size is identical to the size of the grid we used to measure potentials in lab, with one position for each measured potential. The code then moves through each position in the matrix using a pair of nested loops – one to translate through the x dimension, and one to translate through the y dimension. At each position, it uses the solution to Laplace's equation to calculate a potential and store the value in the appropriate position in the matrix. Then, with another pair of nested loops, it writes the values of the matrix into a .txt.

After organizing the data, we create three plots in order to compare the the experimental ones:

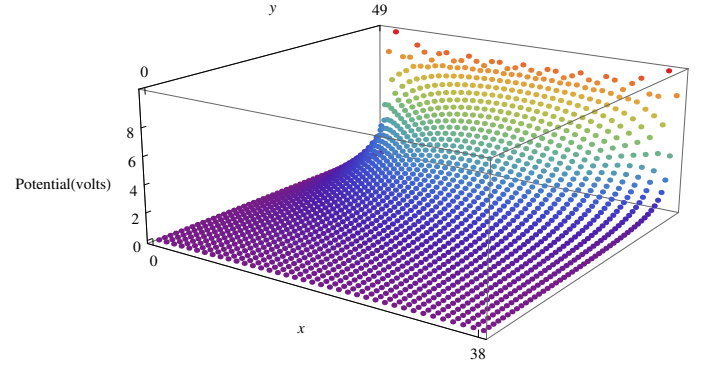


FIG. 7. Analytical list plot

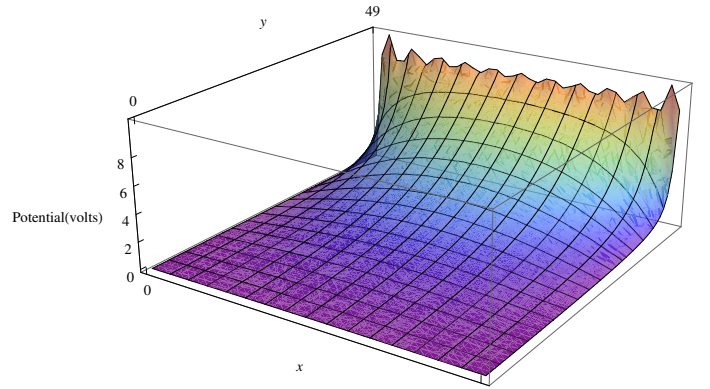


FIG. 8. Analytical surface plot

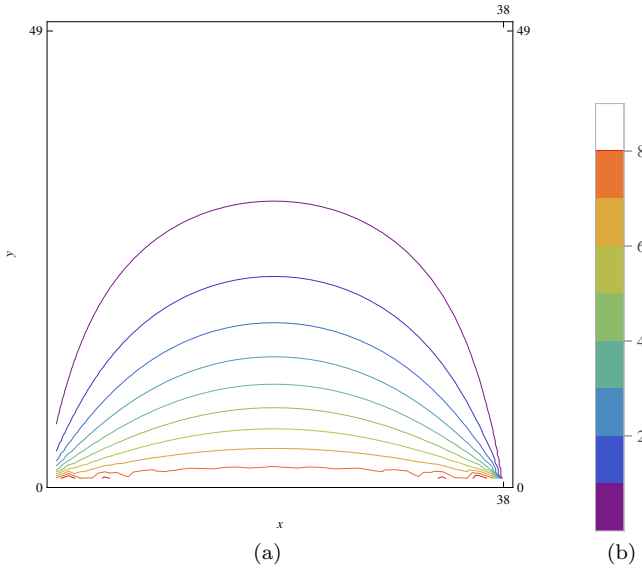
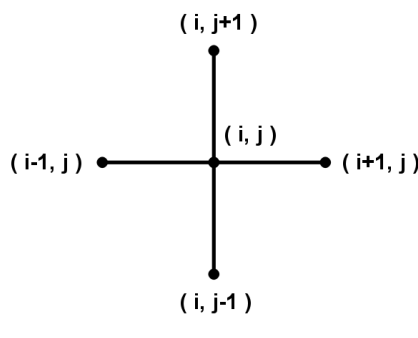


FIG. 9. Analytical contour plot

IV. NUMERICAL METHOD

A. Theory

In order to use the numerical method to solve the Laplace equation, we first utilize the method known as the finite difference method. The purpose of this is to create a system of equations that approximate the value of the potential at the gridpoints when solved. We then use the Jacobi iterative method in order to solve said equations. To create this system of equations, we consider an arbitrary point on the grid with coordinates (i, j) . Any given point away from the boundaries will have four adjacent neighboring points, so we neglect those points that exist without four neighbors for now (FIG 10).

FIG. 10. A gridpoint (i,j) and its four adjacent neighbors

Assuming that these adjacent points are relatively close to one another, then the value of the potential at each point is approximately the average of the value of its four neighbors

$$V_{i,j} = \frac{V_{i,j} + V_{i,j+1} + V_{i-1,j} + V_{i+1,j}}{4} \quad (40)$$

In order to prove the fact that this is a reasonable approximation, we Taylor expand for V_{i-1} and V_{i+1} . If we let these two points be separated on the x axis by a value h , then the expansions are as follows:

$$\begin{aligned} V_{i-1} &= V_i - \frac{\partial V}{\partial x}|_i h + \frac{\partial^2 V}{\partial x^2}|_i \frac{h^2}{2!} - \frac{\partial^3 V}{\partial x^3}|_i \frac{h^3}{3!} \\ &\quad + \frac{\partial^4 V}{\partial x^4}|_i \frac{h^4}{4!} + O(h^5) \end{aligned} \quad (41)$$

$$\begin{aligned} V_{i+1} &= V_i + \frac{\partial V}{\partial x}|_i h + \frac{\partial^2 V}{\partial x^2}|_i \frac{h^2}{2!} + \frac{\partial^3 V}{\partial x^3}|_i \frac{h^3}{3!} \\ &\quad + \frac{\partial^4 V}{\partial x^4}|_i \frac{h^4}{4!} + O(h^5) \end{aligned} \quad (42)$$

where $|_i$ is standard notation for evaluation at the i^{th} point. If we add Eq. 41 and Eq. 42, we obtain

$$V_{i-1} + V_{i+1} = 2V_i + \frac{\partial^2 V}{\partial x^2}|_i h^2 + \frac{\partial^4 V}{\partial x^4}|_i \frac{h^4}{12} + O(h^5) \quad (43)$$

Rearranging Eq. 43

$$\frac{\partial^2 V}{\partial x^2}|_i = \frac{V_{i-1} + V_{i+1} - 2V_i}{h^2} + O(h^2) \quad (44)$$

The RHS of Eq. 44 is the second-order accurate finite difference approximation. If we subtract Eq. 41 from Eq. 42, we obtain

$$V_{i-1} - V_{i+1} = 2\frac{\partial V}{\partial x}|_i h + \frac{\partial^3 V}{\partial x^3}|_i \frac{h^3}{3} + O(h^5) \quad (45)$$

Rearranging Eq. 45

$$\frac{\partial V}{\partial x}|_i = \frac{V_{i-1} - V_{i+1}}{2h} + O(h^2) \quad (46)$$

The RHS of Eq. 46 is the second-order accurate finite difference approximation. We can follow a similar procedure along the y axis to obtain

$$\frac{\partial^2 V}{\partial y^2}|_j = \frac{V_{j+1} + V_{j-1} - 2V_j}{h^2} + O(h^2) \quad (47)$$

and

$$\frac{\partial V}{\partial y}|_j = \frac{V_{i+1} - V_{i-1}}{2h} + O(h^2) \quad (48)$$

By combining Eq. 44 and Eq. 47, we find that

$$\left(\frac{\partial^2 V}{\partial x^2} + \frac{\partial^2 V}{\partial y^2} \right) |_{i,j} = \frac{V_{i+1,j} + V_{i-1,j} - 2V_{i,j}}{h^2} + \frac{V_{i,j+1} + V_{i,j-1} - 2V_{i,j}}{h^2} \quad (49)$$

Substituting Eq. 49 into the Laplace equation, Eq. 5 we find that

$$V_{i+1,j} + V_{i-1,j} - 2V_{i,j} + V_{i,j+1} + V_{i,j-1} - 2V_{i,j} = 0 \quad (50)$$

Rearranging Eq. 50

$$V_{i,j} = \frac{V_{i,j-1} + V_{i,j+1} + V_{i-1,j} + V_{i+1,j}}{4} \quad (51)$$

Q.E.D. Now that we have obtained the system of equations, we must apply the Jacobi iteration method by specifying our given Dirichlet boundary conditions and setting the potential values of all points within the boundary to zero. We can then describe the voltage at some arbitrary i, j after k iterations

$$V_{i,j}^k = \frac{V_{i,j-1}^{k-1} + V_{i,j+1}^{k-1} + V_{i-1,j}^{k-1} + V_{i+1,j}^{k-1}}{4} \quad (52)$$

where we can iterate by k an arbitrarily large amount of times.

B. Application

Proceeding in a similar fashion to the analytical method, we wrote a Fortran code that performs the iteration in Eq. 52. The code begins by creating a two-dimensional array to act as our potential gradient. We based the size of this array on the size of the grid used to measure potentials in the lab – one position in the array for each measured potential. Then we expand the dimensions by two along the x axis and two along the y axis. These new spaces will be used to store V_0 in the first row, and surround the rest of the matrix with the ground, where potential is zero. We use a do loop to set all values in the first row to V_0 , and ensure the grounded regions remain zero by not altering values at the edge of the matrix. Then, in a series of nested loops, the code moves through all positions in the matrix bounded within the ground and initial voltage, and calculates a potential using the numerical method, which is simply the average of potentials surrounding that position. By repeating this process for the entire matrix enough times, the program should converge on the correct gradient. Then to output this data, we use another pair of nested loops to write all positions in the matrix bounded by V_0 and the ground into a .txt.

After organizing the data, we create three plots in order to compare the experimental ones:

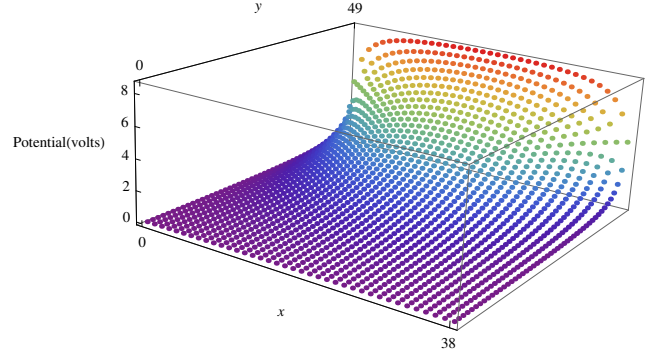


FIG. 11. Numerical list plot

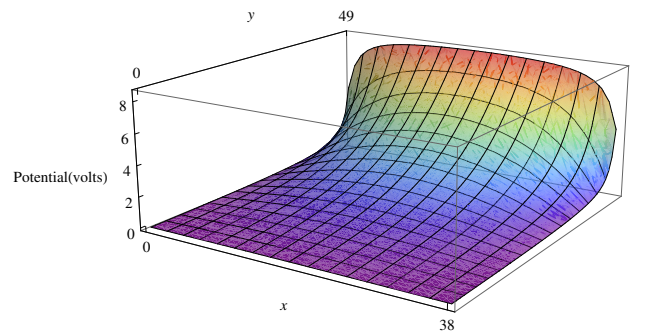


FIG. 12. Numerical surface plot

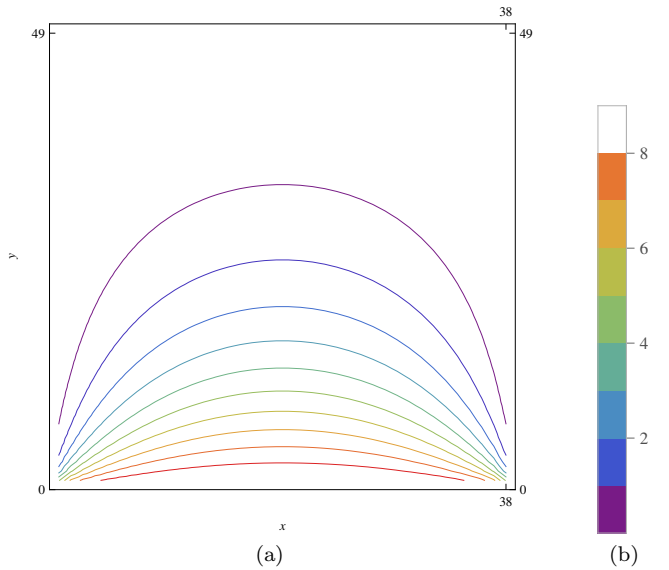


FIG. 13. Numerical contour plot

V. CONCLUSION

Although we have not completely proven that the experimental, analytical, and numerical methods agree with one another, it is not unreasonable to argue that from (FIG 14), our results imply agreement. The three sets of overlayed contour lines show only a small deviation from one another. The two methods with the least amount of deviation from each other are, unsurprisingly, the analytical and numerical methods. This is due to the fact that the uniqueness theorem guarantees a single solution to the Laplace equation inside of our two-dimensional domain. The slight disagreement between the two is likely due to some type of coding error. For the numerical method, the Fortran code sums over an index of $k = 10,000$, while we were only able to sum over an index of $n = 21$ for the analytical Fortran code. We see by looking at (FIG 14) that the experimental contour lines seem to move further apart from theory at the bottom of the experiment. As we move further away from V_0 , the potential drops off, and the voltmeter reaches a point of diminishing returns. This is due in part to the limited accuracy of the voltmeter on small scales. At these small potential scales, the fluctuations of voltage in

the ground start to dominate, resulting in a random reading on the voltmeter. In general, the difference between the experimental and theoretical contour lines are due to the lab setup. The carbon paper has imperfections, and there is internal resistance within the circuit, both of which result in a net displacement of the experimental lines. The experimental data could have easily been improved by any number of changes to the setup that would reduce uncertainty, such as increasing the amount of data points taken, as well as the number of times each point is probed. Overall, given the circumstances of this experiment, we report that the analytical and numerical methods for finding a solution to the Laplace equation are equally valid ways of finding the potential values we directly measured in the laboratory.

ACKNOWLEDGEMENT

We would like to thank the State University of New York at Stony Brook, Department of Physics, and Prof. Eden Figueroa, for providing the necessary lab equipment for this experiment, the American Physical Society for providing and assisting us with the REVTEX 4.1 packages, and Terre Arena of the American Physical Society for proofreading this manuscript.

-
- [1] Griffiths, David J. *Introduction to Electrodynamics*. 4th ed. Prentice Hall 2013.
 - [2] Mitra, A. K. *Finite Difference Method for the Solution of Laplace Equation*. Department of Aerospace Engineering, Iowa State University.
 - [3] *Scheme-it*. Vers. 0.1. Thief River Falls, MN: Digi-Key Electronics, 2015. Online Diagramming Tool.

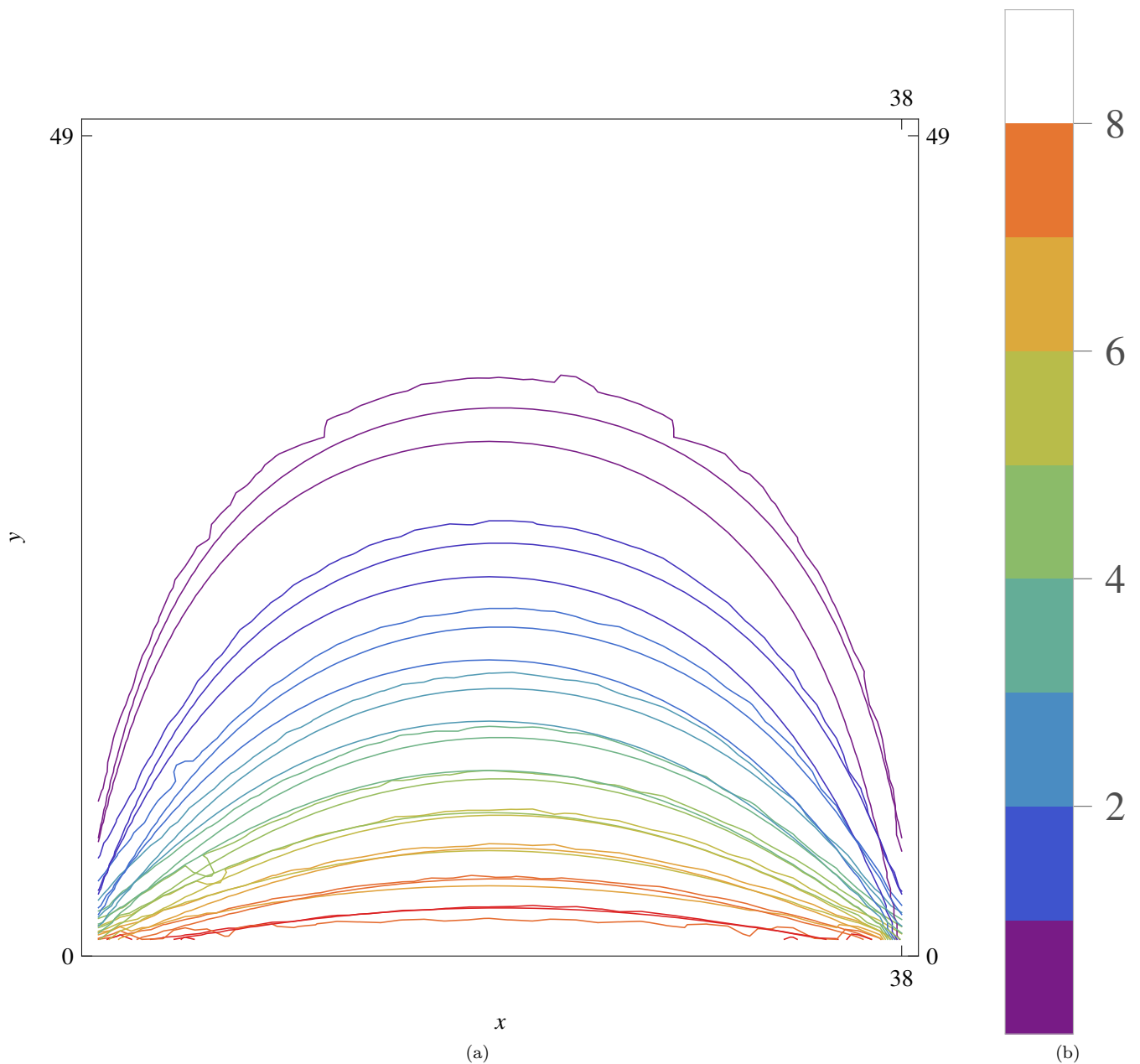


FIG. 14. Analytical vs. Numerical vs. Experimental